Electric Power Systems Research 202 (2022) 107598

Contents lists available at ScienceDirect

Electric Power Systems Research

journal homepage: www.elsevier.com/locate/epsr

Dynamic under-voltage load shedding scheme considering composite load modeling

Ardiaty Arief [a,b,*], Muhammad Bachtiar Nappu [a,b], Zhao Yang Dong [c]

[a] Centre for Research and Development on Energy and Electricity, Hasanuddin University, Jl. Perintis Kemerdekaan Km. 10 Tamalanrea, Makassar 90245, Indonesia
[b] Department of Electrical Engineering, Faculty of Engineering, Hasanuddin University, Poros Malino Km. 6, Bontomarannu, Gowa 92172, Indonesia
[c] School of Electrical Engineering and Telecommunications, the University of New South Wales, Sydney, Kensington, NSW 2052, Australia

ARTICLE INFO

Keywords:
Dynamic load modeling
Dynamic voltage curve sensitivity
Under-voltage load shedding
Voltage stability
Voltage stability margin

ABSTRACT

This manuscript recommends an under-voltage load shedding scheme based on the sensitivity of dynamic voltage curves to mitigate voltage collapse in highly stressed power systems. The developed method can be used to determine the minimum amount and proper locations of load curtailment by considering power system dynamics including dynamic load modeling. The selected Indonesian regional system has a large number of dynamic loads in form of air conditioning and water pump loads whose dynamics contribute considerably to the complexity of the power system stability. Loss of the transmission line in the system caused by the impact of the composite load after major disturbance is studied. The proposed scheme involves an iterative procedure based on the sensitivity analysis of the dynamic voltage curve to solve the problem of load shedding. Furthermore, this work developed a new index named dynamic voltage-active power sensitivity (DVPS). The DVPS is calculated in all load buses to give information about the bus that has a predominant influence on improving system voltage stability through load shedding. Dynamic simulations are carried out with an Indonesian power system, the South Sulawesi interconnection power system with the proposed load shedding scheme. The results of this work show a noteworthy improvement in the magnitude of the voltage level as well as the voltage stability margin.

1. Introduction

1.1. Background and motivations

Since the last century, the stability of the electric power system has been believed as an important precondition for a secure and stable operation of the power system [1]. As the power system expands to a more complex and highly stressed system, with the increasing number of interconnections, renewable energy resources integration, direct current transmission system as well as electricity market, the problem of voltage stability also becomes more crucial, since the stability characteristics of the system become more complicated than before [2]. During the power system scheduling and operation, the problem of voltage stability has been of major interest, due to the considerable amount of system failures caused by voltage instability which is usually caused by a power outage or a sudden increase in load. There are two common defense measures to prevent voltage instability, namely preventive measures, and corrective measures. Preventive measures are taken in a pre-contingency state to improve the margin of voltage security, while corrective measures are usually carried out during post-interference configurations to reinstate system stability. Among the various precautions that can be implemented to preclude voltage instability, under-voltage load shedding (UVLS) becomes more acceptable as an inexpensive and reliable corrective measure. Nevertheless, the UVLS must be the final remedial defense when no other alternative is available to prevent the possibility of a voltage collapse. UVLS plays an important role in power system control and stability when the system is experiencing major disruptions.

The load shedding design must be "robust". The UVLS design must cover sufficient load to be shed but simultaneously not be over-sensitive. The philosophy of UVLS is that if there is a disturbance in the system and the voltage drops to a certain predetermined level within a certain period then a predetermined amount of load is shed from the system [3]. The purpose is that the system voltage returns to its stability limit when a certain amount of load is disconnected from the system.

Research and experience have proven that UVLS is an excellent countermeasure against voltage instability. In this part, we will provide a brief overview of UVLS using the IEEE 14 bus Reliability Test System as shown in Fig. 1 as an example. It is assumed that there is an outage between bus 6 and bus 13. Fig. 2 (a) and (b) show the voltage drop after

* Corresponding author.
E-mail addresses: ardiaty@eng.unhas.ac.id, ardiaty@engineer.com (A. Arief).

https://doi.org/10.1016/j.epsr.2021.107598
Received 20 February 2021; Received in revised form 2 May 2021; Accepted 14 September 2021
Available online 24 September 2021

Nomenclature

DVPS	dynamic voltage-active power sensitivity
UVLS	under-voltage load shedding
VSM	voltage stability margin
$E_d^{'}$	*d*-axis stator transient voltage related to rotor transient flux component
$E_q^{'}$	*q*-axis stator transient voltage related to rotor transient flux component
E_f^*	field voltage
H	inertia constant
I_d	*d*-axis element of stator current
I_q	*q*-axis element of stator current
$T_{do}^{'}$	*d*-axis transient time constant
$T_{qo}^{'}$	*q*-axis transient time constant
$T_{do}^{''}$	*d*-axis subtransient time constant
$T_{qo}^{''}$	*q*-axis subtransient time constant
T_{FW}^*	extra damping torque in comparison to rotor speed
T_M	mechanical torque
$X_d^{'}$	*d*-axis transient reactance
$X_q^{'}$	*q*-axis transient reactance
$X_d^{''}$	*d*-axis subtransient reactance
$X_q^{''}$	*q*-axis subtransient reactance
X_{ls}	armature leakage reactance
δ	generator rotor power angle
ψ_d	subtransient EMFs as a result of *d*-axis damper flux linkage
ψ_q	subtransient EMFs as a result of *q*-axis damper flux linkage
ω	generator rotor angular speed
ω_s	generator synchronous rotor speed ($2\pi f$)
P_{Li}	active load on the bus *i*
Q_{Li}	reactive load on the bus *i*
P_{Li}^0	active load according to the initial bus voltage
Q_{Li}^0	reactive load according to the initial bus voltage
α_P	constant impedance element of the active load
α_Q	constant impedance element of the reactive load
β_P	constant current element of the active load
β_Q	constant current element of the reactive load
γ_P	constant power element of the active load
γ_Q	constant power element of the reactive load
V_i	actual operating voltage at bus *i*
$P_s(V)$	steady state active power load as function of voltage
$Q_s(V)$	steady state reactive power load as function of voltage
$P_t(V)$	transient active power load as function of voltage
$Q_t(V)$	transient reactive power load as function of voltage
P_d	instantaneous active power
Q_d	instantaneous reactive power
T_p	active power time constant
T_q	reactive power time constant
x_p	active power load state variable
x_q	reactive power load state variable
P_{shed_j}	load shedding quantity on bus *j*
n_k	critical buses number
t_k	instantaneous time
t_s	number of instantaneous time

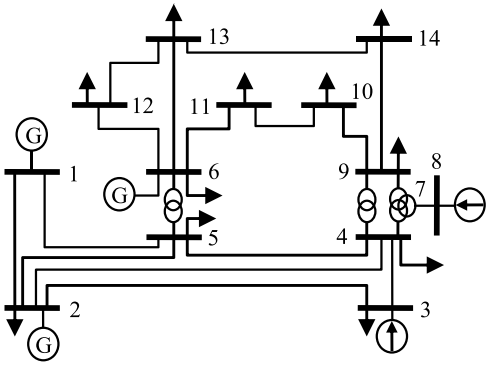

Fig. 1. The IEEE 14 Bus Reliability Test System.

the fault across all buses and the critical buses, respectively. Then Fig. 2 (c) demonstrates the voltage recovery after load shedding.

1.2. State-of-the-art of power system under-voltage load shedding

Various research had been conducted to investigate preventive and corrective actions to preclude instability using voltage stability analysis, which is an imperative instrument for predicting probable instability and generally can be categorized into static, quasi-static, and dynamic voltage stability analysis. In the literature, numerous methods have been utilized to design effective UVLS schemes. Most of them use static or dynamic voltage stability analysis. This section will provide an overview of existing UVLS methods. The authors in [4] developed an optimization model with relaxation restrictions to compute minimal load shedding. A load shedding based on modal participation factors was proposed in [5] to identify load shedding location. The multistage method for deciding the location and minimum amount of load curtailment was presented in [6]. The author in [7] developed UVLS based on integer value modeling and presented the interruption penalty factor for feeders and the participation penalty factor for buses to minimize the total curtailment of the load. A load shedding was designed by using Particle swarm optimization (PSO) in [8]. Teaching learning-based optimization (TLBO) was implemented in [9] for load shedding and the locations for load shedding were determined by using the severity index sensitivity. The work in [10] formulated an improved risk-based AC security-constrained optimal power flow (RB-SCOPF) for load shedding amount. Another OPF based UVLS to determine the amount, place, degree, and timing of load shedding to maintain a predetermined voltage stability margin was proposed by [11] and Linear optimization-based optimal power flow (LP-OPF) for load shedding was suggested by [12]. The work in [13] established load shedding requirements of the extended equal area criterion (EEAC). The authors in [14] recommended a technique for determining load shedding location by taking into consideration multi-contingencies by tracking the stability index and for computing load shedding amount by using a modified fuzzy logic system. Hybrid Imperialist Competitive Algorithm-Pattern Search (HICA-PS) was employed for load shedding in [15]. In paper [16], the authors presented a load shedding scheme by using the eigenvalue of the Jacobian matrix to determine load shedding location and using Genetic Algorithm (GA) and Neural Network (NN) to compute load shedding amount. However, these UVLS schemes were developed based on the static voltage analysis approach. The drawback of the static voltage analysis technique is that it cannot justify the dynamic character of the occurrences of voltage collapse. The static and quasi-static voltage stability analyses are based on the power flow snapshots and these methods do not take into consideration the dynamic modeling of the system. On the other hand, time-domain simulations hold an important role in assessing the voltage collapse phenomena mechanism.

The studies in [17-21] investigated UVLS schemes based on

time-domain simulations. A UVSL based on adaptive model predictive control (MPC) was developed by [17]. A remedial action scheme (RAS) was created in [18] where candidates for load shedding location were ranked according to their categories and influences on the system stability and enactment. The authors in [19] analyzed the impacts of grid behavior with various UVLS schemes. The study in [20] presented a wide area voltage stability index-based load shedding scheme and used a modified Discrete Imperialistic Competition Algorithm (DICA) to solve the load shedding. Even though these studies proposed UVLS based on time-domain simulations, yet in these works, detailed load modeling (static and dynamic load models) are not considered. Nevertheless, load modeling is important and holds a vital part in the assessment of dynamic voltage stability as well as the design of UVLS, hence proper modeling of the load will give a significant impact on the accuracy of the simulation results.

1.3. Contributions of this paper

Based on the discussion above, there were a considerable number of research works that have investigated and proposed different UVLS schemes. However, these studies have no consideration for detailed load modeling and do not fully take into account the system dynamic modeling particularly from the majority proportion of induction motor loads in a power system.

In the modern power system with a substantial quantity of air conditioning loads, with only a static load model in time-domain simulation is inadequate to evaluate the process of voltage collapse. Especially in Indonesia, several systems are featured with significant air conditioning and pumping loads. As the power system becomes profoundly stressed and works at its boundaries with reduced capacity and stability margins, a more precise representation of load characteristics becomes more vital. Instability in a power system with a considerably large quantity of dynamic motor loads can result in slow voltage improvement or rapid voltage drop [22]. The deficiency of dynamic load modeling in the time

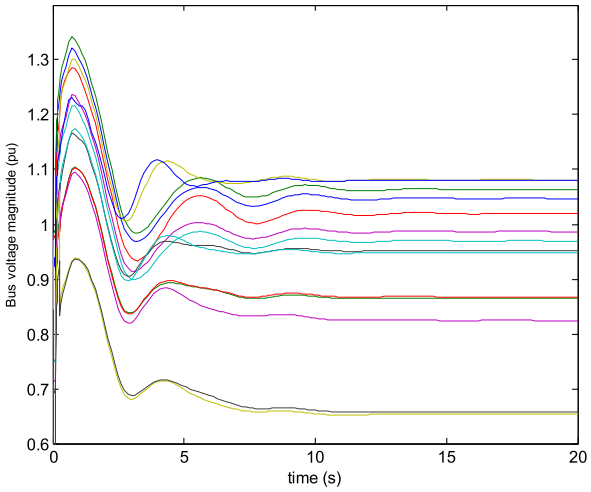

(a) Voltage drop across all buses

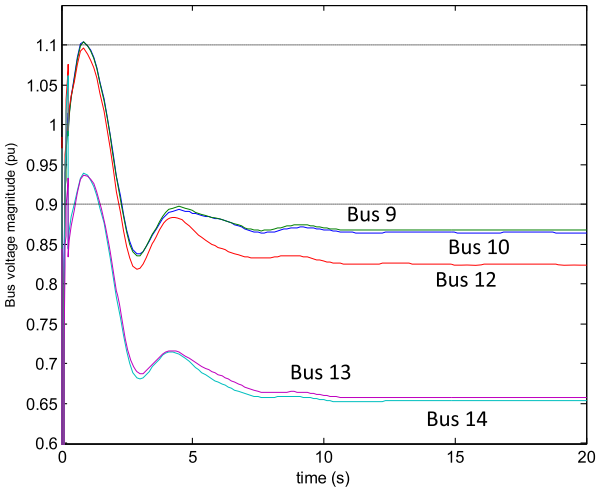

(b) Voltage drop across the critical buses

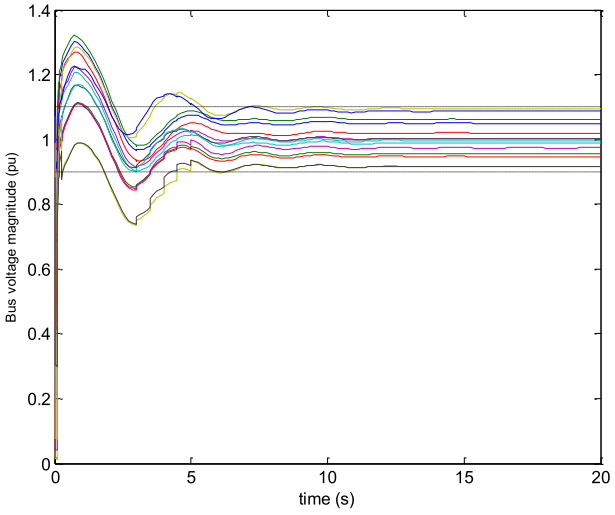

(c) Voltage recovery after load shedding

Fig. 2. Voltage performance after disturbance and load shedding. (a) Voltage drop across all buses (b) Voltage drop across the critical buses (c) Voltage recovery after load shedding.

domain simulation is assumed to be the main reason for the inconsistencies between real measurements and simulation outcomes [23]. Motors have trouble accelerating after main interruptions and can distress voltage profile improvement [24]. Induction motors may stall and draw high currents and result in an increase in voltage drop in some areas in the system. To plan a robust UVLS scheme, it is essential to precisely represent the load model inclusive of induction motors. Therefore, for financial reasons, it is crucial to determine a technique for optimum and more precise load shedding that incorporates dynamic induction motor models.

In this paper, a new analytic and systematic method is suggested to design a strategic under-voltage load shedding scheme that incorporates dynamic voltage sensitivity analysis as an approach for computing the amount and location of load curtailment in a power system. The developed method comprises an iterative procedure that calculates the bus dynamic voltage sensitivities concerning the amount of load shedding. At each stage, the load shedding quantity is set to a small amount of about 1% of the total load. Additionally, a new formulation, namely dynamic voltage-active power sensitivity (DVPS) is created based on dynamic voltage sensitivities to decide the location of load shedding. Furthermore, the proposed UVLS scheme is evaluated based on the voltage stability margin. The amount of load shedding 1% for each iteration is considered sufficient to calculate the total amount of load shedding. However, it is possible to reduce the amount of load shedding per iteration. A more optimal amount of total load shedding can be obtained but more iterations are required. On the other hand, increasing the amount of load shedding per iteration will result in the possibility of a more calculated amount of load shedding than is needed (over shedding).

Therefore, to fulfill this imperative research gap, this work aims to deliver these novel contributions:

i A new UVLS scheme is developed using dynamic voltage stability analysis;
ii Detailed static and dynamic load modeling are considered, and load compositions are included for a more realistic, reliable, and effective UVLS design; and
iii A new formulation of dynamic voltage active power sensitivity (DVPS) is formulated to determine the location and amount of load shedding.

The UVLS method developed in this paper involves multistage or iterative solutions. The main reason for this iterative process is to minimize the load shedding amount by analyzing its dynamic sensitivity with a small amount of load shedding for every iteration until the system is stable hence the optimal or minimum amount for load shedding can be obtained.

The remainder of this paper is organized as follows: Section 2 provides an explanation about power system modeling for the UVLS design. Section 3 outlines the proposed methodology: the dynamic voltage sensitivities enhanced UVLS scheme. Section 4 specifically gives information about the South Sulawesi system in Indonesia. Section 5 provides the results and analysis then Section 6 concludes the research key outcomes. These work results are expected to deliver a better set of UVLS to deal with the possibility of voltage collapse occurrence, particularly in the South Sulawesi power system.

2. Power systems modeling for under-voltage load shedding studies

The first step of dynamic voltage stability assessment is to have a reliable power system model. This includes key elements of a power system, i.e. generators, network, and loads for both steady-state and dynamic. The following section describes the system modeling for the proposed UVLS scheme.

2.1. Synchronous generator modeling

The synchronous generator model employed in this work is the detailed 6th order synchronous machine model. The 6th order synchronous machine model considers four windings with the existence of a field circuit and supplementary circuit by the *d*-axis and two further circuits through the *q*-axis. Nevertheless, the network and stator transients in the 6th order model are ignored. The dynamics generated by these transients are negligible and would give slightly conservative results, which are more suitable for dynamic analysis, predominantly for fast screening to identify and recognize all critical and unstable consequences [25]. In dynamic voltage stability, the differential equations overseeing the sub transient behavior of the 6th order synchronous machines are given by the following equations [26],

$$T'_{do}\frac{dE'_q}{dt} = -E'_q - (X_d - X'_d)\left[I_d - \left(\frac{X'_d - X''_d}{(X'_d - X_{ls})^2}\right)\left\{\psi_d + (X'_d - X_{ls})I_d + E'_q\right\}\right] + E^*_f \tag{1}$$

$$T''_{do}\frac{d\psi_d}{dt} = -\psi_d + E'_q - (X'_d - X_{ls})I_d \tag{2}$$

$$T'_{qo}\frac{dE'_d}{dt} = -E'_d + (X_q - X'_q)\left[I_q - \left(\frac{X'_q - X''_q}{(X'_q - X_{ls})^2}\right)\left\{\psi_q + (X'_q - X_{ls})I_q + E'_d\right\}\right] \tag{3}$$

$$T''_{qo}\frac{d\psi_q}{dt} = -\psi_q + E'_d - (X'_q - X_{ls})I_q \tag{4}$$

$$\frac{d\delta}{dt} = \omega - \omega_s \tag{5}$$

$$\frac{2H}{\omega_s}\frac{d\omega}{dt} = T_M - \left(\frac{X''_d - X_{ls}}{X'_d - X_{ls}}\right)E'_q I_q - \left(\frac{X'_d - X''_d}{X'_d - X_{ls}}\right)\psi_d I_q - \left(\frac{X''_q - X_{ls}}{X'_q - X_{ls}}\right)E'_d I_d + \left(\frac{X'_q - X''_q}{X'_q - X_{ls}}\right)\psi_q I_d - (X''_q - X''_d)I_d I_q - T^*_{FW} \tag{6}$$

2.2. Load modeling

Load modeling is crucial and one of the most important elements in the dynamic voltage stability analysis included in the UVLS design. In this study, the load on each bus is demonstrated as a composite load model which is a combination of static and dynamic load components. Section 5 elaborates further details of the load configuration in this work. Fig. 3 shows the equivalent circuit of the composite load model, where Z is constant impedances; I is constant currents; P is constant powers; X_m is the magnetization reactance; X_s is the stator leakage reactance; X_r is the rotor leakage resistance; R_s is the stator resistance; R_r

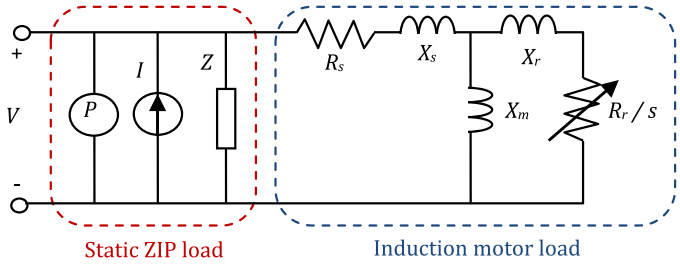

Fig. 3. Schematic circuit of the composite load model [27].

is the rotor resistance, and s is the induction motor slip.

2.2.1. Static load modeling

In general, loads depend on the voltage of a bus. Static load voltage reliance can be stated through exponential or polynomial equations. Static ZIP load modeling is commonly expressed as a voltage magnitude function on a particular bus connected to the load as [28],

$$P_{Li}(V_i) = P_{Li}^0\left[\alpha_P\left(\frac{V_i}{V_0}\right)^2 + \beta_P\left(\frac{V_i}{V_0}\right) + \gamma_P\right] \tag{7}$$

$$Q_{Li}(V_i) = Q_{Li}^0\left[\alpha_Q\left(\frac{V_i}{V_0}\right)^2 + \beta_Q\left(\frac{V_i}{V_0}\right) + \gamma_Q\right] \tag{8}$$

2.2.2. Dynamic load modeling

Dynamic load modeling is essential for UVLS strategy since induction motors will slow down substantially when their terminal voltage declines because of short circuits. The common models for induction motor type dynamic loads are [29],

$$T_p\frac{dP_d}{dt} + V^{\alpha_t}P_d = V^{\alpha_t}P_s(V) + \alpha_t T_p\frac{P_d}{V}\frac{dV}{dt} \tag{9}$$

$$T_q\frac{dQ_d}{dt} + V^{\beta_t}Q_d = V^{\beta_t}Q_s(V) + \beta_t T_q\frac{Q_d}{V}\frac{dV}{dt} \tag{10}$$

where α_t, α_s, β_t, β_s, P_1 and Q_1 are constants independent of load busbar voltage V.

3. Dynamic voltage sensitivities enhanced UVLS scheme

3.1. Dynamic voltage active power sensitivity analysis

The dynamic voltage active power sensitivity analysis is developed based on the dynamic voltage curve sensitivity analysis which is a method based on the linearization of the system that surrounds a particular tracking and utilizes time-domain simulations, which differs from the P-V curves that are usually used in steady-state voltage stability analysis. This process calculates the sensitivity of the dynamics associated with constraints. Dynamic sensitivity can enumerate fluctuations in system variables in correlation to rapid alterations in system parameters and initial conditions. Computation of these sensitivities-based analyses can be found in [30] and discussed briefly below for completeness.

A power system model can be demonstrated by the following differential-algebraic equations (DAEs) for a systematic voltage stability analysis:

$$\dot{x} = f(x, y; \alpha) \tag{11}$$

$$0 = g(x, y; \alpha) \tag{12}$$

where x represents dynamic variables vector; y denotes algebraic variables vector such as voltage magnitudes and angles of the load bus, and α symbolizes system constraints/parameters.

The paths of (11) and (12) demonstrate the dynamic variables x and algebraic variables y performances, where movements of variables x and y can be expressed as,

$$x(t) = \phi_x(x_0, t, \alpha) \tag{13}$$

$$y(t) = \phi_y(y_0, t, \alpha) \tag{14}$$

The Taylor series expansion is implemented in the above equations to acquire the movement sensitivities of ϕ_x and ϕ_y to the original situations and parameter changes, hence

$$\Delta x(t) = \Delta\phi_x(x_0, t, \alpha) = \frac{\partial\phi_x(x_0, t, \alpha)}{\partial\alpha}\Delta\alpha = \frac{\partial x(t)}{\partial\alpha}\Delta\alpha \cong x_\alpha(t)\Delta\alpha \tag{15}$$

$$\Delta y(t) = \Delta\phi_y(y_0, t, \alpha) = \frac{\partial\phi_y(y_0, t, \alpha)}{\partial\alpha}\Delta\alpha = \frac{\partial y(t)}{\partial\alpha}\Delta\alpha \cong y_\alpha(t)\Delta\alpha \tag{16}$$

The sensitivities of x_α and y_α are computed by using an approximate numeric method, consequently

$$x_\alpha = \frac{\partial x}{\partial\alpha} = \frac{\Delta x}{\Delta\alpha} \approx \frac{\phi_x(x_0, t, \alpha + \Delta\alpha) - \phi_x(x_0, t, \alpha)}{\Delta\alpha} \tag{17}$$

$$y_\alpha = \frac{\partial y}{\partial\alpha} = \frac{\Delta y}{\Delta\alpha} \approx \frac{\phi_y(y_0, t, \alpha + \Delta\alpha) - \phi_y(y_0, t, \alpha)}{\Delta\alpha} \tag{18}$$

3.2. The dynamic voltage-active power sensitivity (DVPS) formulation and research algorithm

The dynamic sensitivities of (16) and (18) are modified to encounter the main intention of this research. Although the Q-V curve is normally used for voltage stability assessment, however, to have a more straightforward indicator for direct load-shedding decision making, it is more convenient to have an indicator associated with active power (P). Therefore, we proposed the UVLS design by assessing the degree of change in voltage magnitude regarding the degree of change in active power. The variable y represents the bus voltage magnitude and the load shedding amount are denoted by α, then the bus voltage variation sensitivities after load shedding on a particular bus are calculated as,

$$\Delta V(t) = \Delta\phi_V(V_0, t, P) = \frac{\partial\phi_V(V_0, t, P)}{\partial P}\Delta P = \frac{\partial V(t)}{\partial P}\Delta P \cong V_P(t)\Delta P \tag{19}$$

$$\phi V_P = \frac{\partial V}{\partial P} = \frac{\Delta V}{\Delta P} \approx \frac{\phi_V(V_0, t, P + \Delta P) - \phi_V(V_0, t, P)}{\Delta P} \tag{20}$$

The dynamic sensitivities are calculated to obtain the location of load shedding as well. A dynamic voltage-active power sensitivity (DVPS) is formulated to provide information about the participation of bus j after load shedding on bus j with a predefined amount to the enhancement of the system voltage stability. The premeditated sensitivity is $[\partial V_i/\partial P_j]$, which expresses the degree of voltage magnitude variations on the bus i with the changes in load shedding amount on bus j. The DVPS on bus j is calculated by curtailing active power on bus j by a small quantity then evaluates its effect on all critical buses voltage magnitudes along with time domain, hence the DVPS is formulated as,

$$DVPS_j = \sum_{i=1}^{n_k}\left[\sum_{t=0}^{t_s}\left[\frac{\partial V_i}{\partial P_j}\right]_{t=t_k}\right] \tag{21}$$

$$\partial P_j = \Delta P_j = P_{shed_j}$$

Where t_k is the instantaneous time which is the time instant throughout the time domain simulation where the sensitivity value $[\partial V_i/\partial P_j]$ is recorded to calculate DVPS and t_s is the number of instantaneous time which is the total of all the time instant where $[\partial V_i/\partial P_j]$ is recorded.

The bus with the highest DVPS has the predominant influence in improving the system voltage stability on the critical buses based on time-domain analysis, therefore this bus is chosen as a candidate for load shedding location. For better understanding, the stages for determination of the amount and location of load shedding are illustrated through the flowchart in Fig. 4 whereas the computational procedures are explained in detail below:

Step 1 Set of the load shedding quantity. In this research, the load shedding quantity is arranged at 1 % of the total load for each iteration.
Step 2 Determination of a predefined set of contingencies, then selects a fault.
Step 3 Execution of dynamic voltage stability analysis or time-domain simulation analysis to examine the voltage behavior for all buses in case of unforeseen circumstances. In this stage, the post-fault

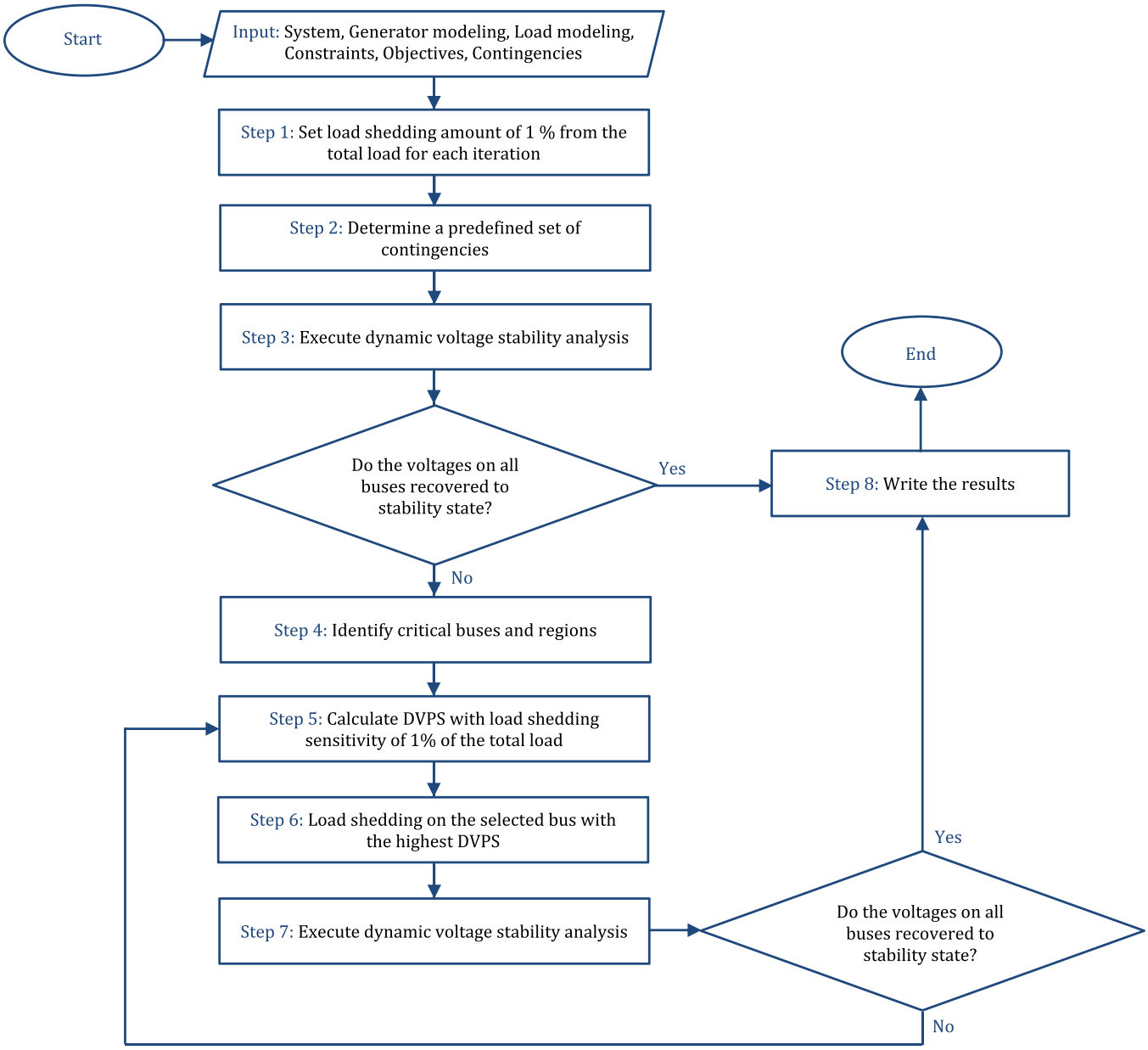

Fig. 4. Flowchart of the proposed UVLS scheme.

voltage recovery on all buses is checked whether they are within the stability limit. If so, the process terminates. Otherwise, it indicates that the system needs load shedding to avoid possible voltage collapse, then go to *Step 4*.

Step 4 Identification of critical buses and regions. The critical region is the region where neighboring buses experience voltage drop below the stability limit and they have similar voltage drop trajectory.

Step 5 Calculation of DVPS using Eq. (21) to evaluate the influence of each load bus in the voltage stability recovery of the buses within the critical areas with load shedding quantity of 1% of the total load. The bus with the highest DVPS means that this bus is the most sensitive bus therefore it has the main influence on increasing the voltage magnitude with a small amount of load shedding. The location of load shedding is determined based on the highest DVPS value.

Step 6 Application of load shedding on the designated bus with the highest DVPS.

Step 7 Execution of dynamic voltage stability analysis to assess system operation after load shedding. At this point, further examinations are carried out to identify whether the post-fault voltage recovery performance on all load buses after load shedding satisfies the voltage stability constraints. If yes, the workflow proceeds to *Step 8* to conclude the process and write the results. Else, it indicates more load shedding, hence the framework switches to *Step 5*.

Step 8 Completion of dynamic UVLS scheme process, write the results and stop the process.

3.3. Stability constraints, optimization objective, and voltage stability margin

In order to meet the voltage stability criteria, the following voltage stability constraints are used:

$$0.9 \leq V_{(t_{k+N})} \leq 1.1 \tag{22}$$

Furthermore, the optimization objective of the dynamic curve sensitivity UVLS is to determine the minimum quantity of load shedding

to ensure voltage constraints are met, then

$$\min \sum_{j=i}^{m} P_{shed_j} \tag{23}$$

where m is the number of load shedding locations.

The voltage stability margin (VSM) is computed by using the PV curve methods [5]. VSM is stated as the growth of the total load in the region of load addition which is calculated from the base case state to the maximum power transfer (PV curve nose point) signified in MW or percentage. The VSM can be computed with this relation

$$VSM\ (\%) = \frac{\lambda_k^{max} - \lambda_{base}}{\lambda_k^{max}}\ \text{x}\ 100\% \tag{24}$$

where λ_{base} is the basic loading parameter for basic case operations and λ_k^{max} is the maximum loading parameter for particular circumstances.

4. The test system: South Sulawesi power system

4.1. Overview of the study system [31]

The South Sulawesi interconnection power system comprises various power plants interconnected by several high voltage transmission lines with the provincial capital of Makassar City. The South Sulawesi system has a typical feature where the main cost-effective power plants are positioned in the north of the system, whereas the major load center is found in the south. The total power generation in the northern part of the system is 384.9 MW whereas the total generation in the southern part is 232.7 MW. The Total peak load of the system for the case study was 556.5 MW.

The load in the South Sulawesi system is dominated by the residential load. As a center of provincial government and business, the load in Makassar City (which is the capital of the South Sulawesi province, business center for eastern Indonesia represented by buses 10, 11, 12, and 13) is dominated by dynamic loads which are commonly air conditioner and water pump loads. In addition, two large cement industries are connected to bus 8. Fig. 5 presents the single-line diagram of the case study system.

4.2. Load composition

In this study, the load is presumed to be peak load. In the provincial capital, Makassar, (buses 10, 11, 12, and 13), the load is represented as 50% static load and 50% dynamic load, because Makassar is the province's business center and its residents are generally in the middle and upper economic levels. Fig. 6 shows the assumption of the load illustration in Makassar. On other buses, the load is considered as 80% static load and 20% dynamic load, with an exception, on bus 8, where there are two large cement industries connected, the load is depicted as 30% static load and 70% dynamic load. Detail of the system load composition and parameters of induction motors [23] are presented respectively in Tables 1 and 2.

Where Type I Weighted cumulative of residential motors
Type II Weighted cumulative of air conditioning dominant motors
Type III Water pump
Type IV Large industrial induction motors

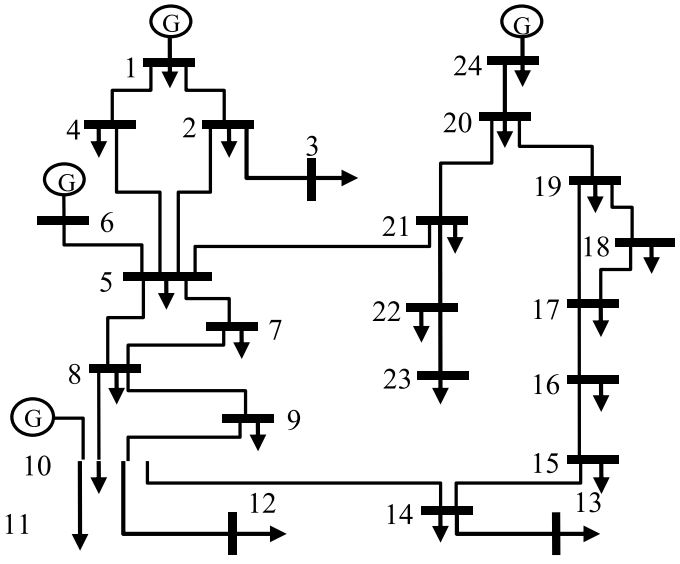

Fig. 5. The single-line diagram of the case study [31].

5. Case study and analysis

Since the total load is 556.5 MW, therefore the load shedding amount for each DVPS computation is set at 1% or about 5 MW. The case observed in this case study was an outage between buses 8 and 10 since it resulted in a severe voltage collapse situation.

Fig. 7 shows the voltage collapse after a disturbance has occurred which causes the loss of the transmission line between buses 8 and 10. Because of this outage, there are 3 unstable regions detected: Makassar City region (buses 10 - 14), buses 8 and 9; and buses 22 and 23 where the voltage collapse in these regions are shown in Figs. 8-10 respectively. Specifically from Fig. 8, this clearly illustrates a substantial voltages drop in the Makassar substations which drop to the voltage of 0.66 – 0.69 p.u. at time t=30 s. This is because Makassar as the load center in the South Sulawesi system has a significantly large quantity of dynamic induction motor loads. Because induction motors have trouble accelerating after big perturbance then they stall and distress the voltage in the Makassar region.

In this simulation, the voltage stability constraint is violated, therefore load shedding is required to retrieve stability. Dynamic sensitivity analysis is carried out to evaluate the impact of 5 MW load shedding on each load bus in the critical unstable region. For illustration, we took bus 13 and 3 as examples to calculate the DVPS value. Since there are 9 unstable buses (buses 8, 9, 10, 11, 12, 13, 14, 22, and 23), hence we only analyzed the sensitivity of 5 MW load shedding on those unstable buses. Figs. 11 and 12 illustrate the sensitivities of the dynamic voltage curve of the mentioned unstable buses for the first iteration of 5 MW load shedding is applied to bus 13 and bus 3, respectively. It can be concluded from both figures, that the sensitivity of the dynamic voltage curve for the 5 MW load shedding on bus 13 is better than the dynamic voltage curve sensitivity for the 5 MW load shedding on bus 3. Furthermore, DVPS as defined in Eq. (21) is computed to present a distinctive indicator for the location of load shedding. The results of calculation $\sum_{t=0}^{t_s}\left[\frac{\partial V_i}{\partial P_j}\right]_{t=t_k}$ with respect to all unstable buses to calculate DVPS on buses 13 and 3 are shown in Table 3. The DVPS values for buses 13 and 3 are calculated based on the sensitivities in Figs. 11 and 12, respectively.

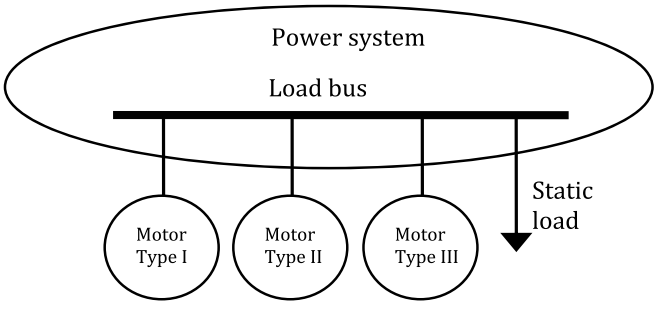

Fig. 6. Assumption of a schematic representation of load at Makassar City region.

Table 1
Load Composition

Bus No	Load type (%)				
	Static	Dynamic motor			
		I	II	III	IV
1 – 7, 9, 14-24	80	20	-	-	-
8	30	20	-	-	50
10 - 13	50	20	25	5	-

Table 2
Induction Motor Parameters [23]

Motor type	I	II	III	IV
Stator resistance - R_s	0.077	0.064	0.013	0.013
Stator leakage reactance – X_s	0.107	0.091	0.14	0.067
Magnetizing reactance - X_m	2.22	2.23	2.4	3.8
Rotor resistance - R_r	0.079	0.059	0.009	0.009
Rotor leakage resistance - X_r	0.098	0.071	0.12	0.17
Rotor inertia constant - H	0.74	0.34	0.8	1.5
Load factor	0.46	0.8	0.7	0.8

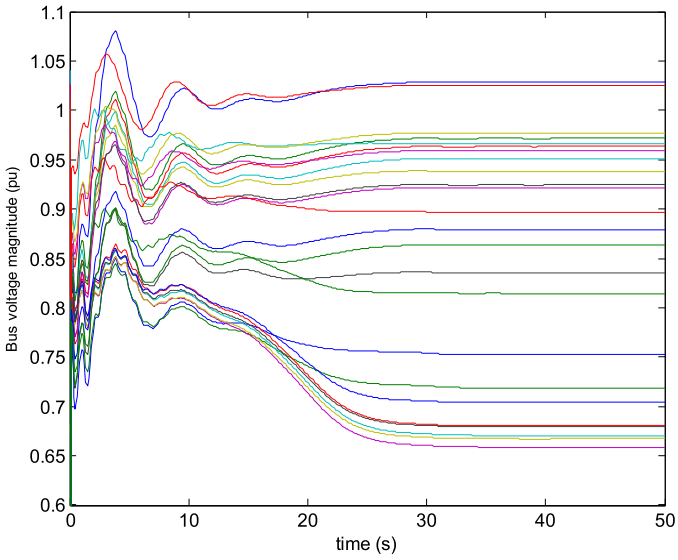

Fig. 7. Voltage declines in all buses after interruptions between buses 8 and 10.

In calculating the DVPS values, we used a time interval of 0.5 seconds for a period of 0 – 10 seconds and 1 second for 10 – 30 seconds. As can be seen in Fig. 7., the voltages fluctuate a lot during the first 10 seconds after the disturbance, change slightly over 10-30 seconds, and tend to remain the same after 30 seconds.

Fig. 13 informs the DVPS value in the first iteration for 5 MW sensitivity in each load bus. As the result, bus 13 has the highest DVPS value (24.92) and it is indicated with a red bar. Load curtailment of 5 MW is evaluated on bus 13 and the system voltage performance is re-assessed. In this phase, the system voltage is not able to improve back to its stability condition, hence the dynamic voltage curve sensitivities are executed again to compute DVPS. For this outage, this process was done in 6 iterations until the constraints are met and the results of DVPS value in each iteration are given in Table 4. Table 5 summarizes the highest DVPS value for each iteration and the buses with the highest DVPS for each iteration. Therefore, we obtained the load shedding locations for this case are buses 13 (15 MW), 9 (5 MW), and 23 (10 MW) and are summarized in Table 6. Fig. 14 shows the results of the voltage enhancement after load curtailment with a total of 30 MW on buses 13, 9 and 23. This verifies that all voltages have significantly improved and the system stability has been retrieved.

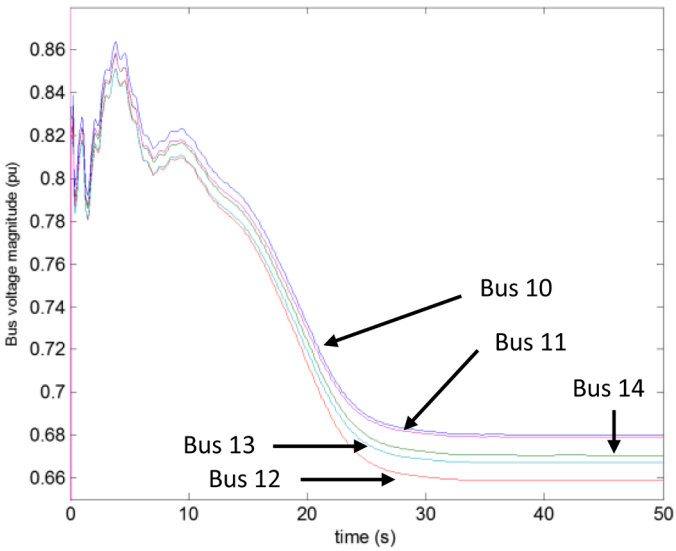

Fig. 8. Voltage declines in buses 10 – 14 after interruptions between buses 8 and 10.

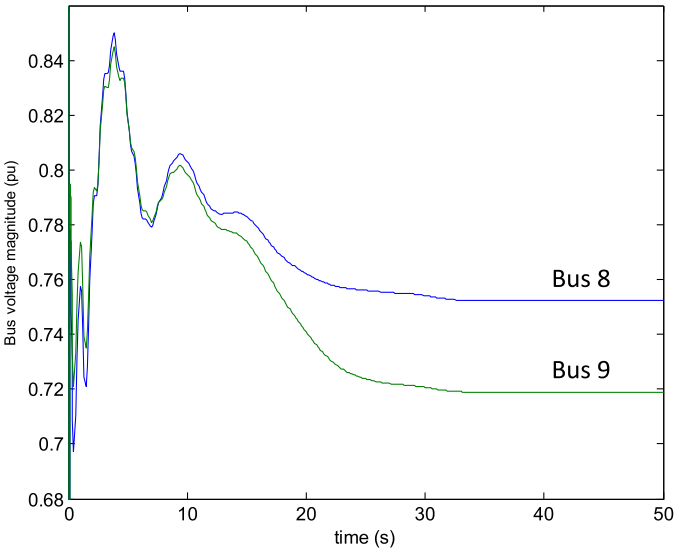

Fig. 9. Voltage declines in buses 8 and 9 after interruptions between buses 8 and 10.

To illustrate the advantage of the proposed scheme, this work observes how the voltage improvement if the load shedding is carried out on bus 13 itself for 30 MW as a comparison because in the first iteration bus 13 has the highest DVPS value. Fig. 15 shows the voltage behavior after 30 MW load shedding on bus 13. It is interesting, even though the voltage magnitude increase but the voltage on buses 8 and 23 cannot return to the stability constraints. Therefore, it is not recommended to shed load on bus 13 by 30 MW, although in the first iteration, bus 13 has the highest DVPS. By assessing the load shedding locations by a smaller amount, can provide a more efficient load shedding scheme.

Furthermore, this work also investigates and compares the proposed load shedding with the South Sulawesi system load shedding scheme. The state electricity provider had a load shedding design with total load shedding of 31.64 MW and was located on buses 19, 22, 4, 2, 3, 24, and 18 as shown in Table 7 [31]. Fig. 16 shows the voltage behavior after load shedding on these buses and confirms that with this arrangement, the system voltage stability cannot recover back to the stability constraints. It can be seen that after the load curtailment, the system voltage

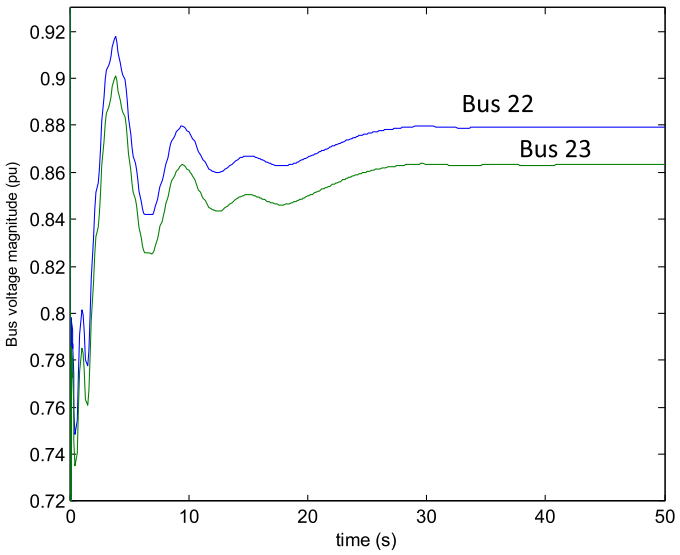

Fig. 10. Voltage declines in buses 22 and 23 after interruptions between buses 8 and 10.

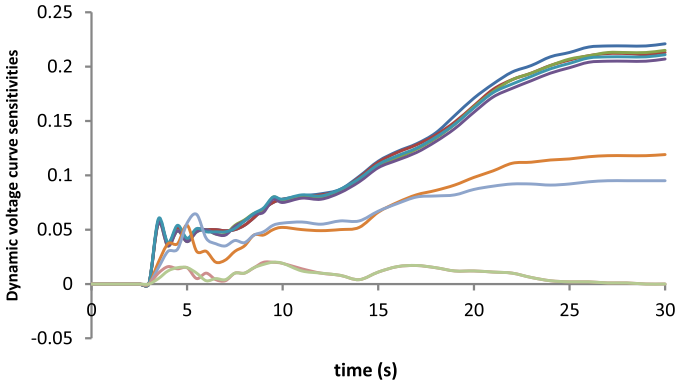

Fig. 11. Dynamic voltage curve sensitivities if a 5 MW load shedding is applied to bus 13.

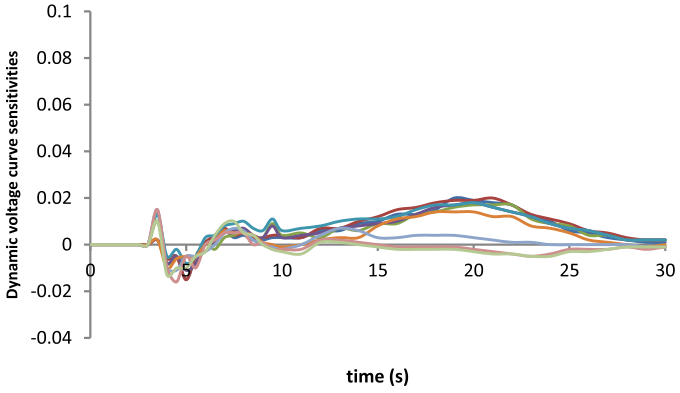

Fig. 12. Dynamic voltage curve sensitivities if a 5 MW load shedding is applied to bus 3.

can slightly increase, but after t=40 s, the voltages in the Makassar region drop significantly to approximately 0.66 p.u. This condition is the same as if there was no load shedding. Therefore, this load shedding scheme is not as effective and efficient as our proposed scheme. Consequently, more load shedding amount is required in order to comply with the system voltage stability constraints and it is not

Table 3
DVPS Calculation

Bus j / Bus i	$\sum_{t=0}^{t_k}\left[\frac{\partial V_i}{\partial P_j}\right]_{t=t_k}$ 13	3
8	2.222	0.038
9	2.352	0.125
10	3.933	0.257
11	3.934	0.184
12	4.051	0.187
13	3.957	0.22
14	3.829	0.188
22	0.314	-0.047
23	0.326	-0.041
DVPS Value	24.918	1.111

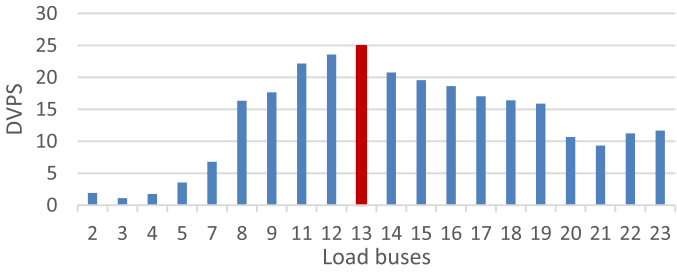

Fig. 13. DVPS value in the first iteration.

Table 4
DVPS Value

Iteration	DVPS I	II	III	IV	V	VI
Bus No						
2	1.91	1.24	1.03	0.87	0.77	0.53
3	1.11	0.97	0.78	0.57	0.46	0.32
4	1.76	1.12	0.98	0.76	0.65	0.44
5	3.56	2.79	2.11	1.95	1.76	1.32
7	6.79	5.35	4.05	3.34	2.56	1.06
8	16.34	14.11	13.33	9.12	6.34	5.12
9	17.66	15.23	**14.12**	9.88	5.65	5.45
11	22.17	18.98	12.56	9.69	1.78	1.56
12	23.57	20.04	13.02	10.03	1.89	1.32
13	**24.92**	**21.32**	13.78	**10.65**	1.12	0.95
14	20.76	17.64	11.45	9.34	1.67	0.65
15	19.57	15.87	10.87	8.67	3.76	2.89
16	18.63	13.96	9.98	7.67	4.78	3.23
17	17.05	12.31	9.02	6.99	4.03	3.54
18	16.4	11.44	8.34	6.12	5.78	3.97
19	15.89	9.98	7.86	5.46	4.78	3.89
20	10.67	7.02	5.79	4.67	3.78	3.08
21	9.34	5.95	4.57	3.56	2.88	2.01
22	11.23	10.28	8.79	8.12	7.65	6.45
23	11.68	10.57	9.86	9.55	**8.78**	**8.12**

Table 5
Highest DVPS Value and Load Shedding Location for each iteration

Iteration	Highest DVPS	Bus (location)
I	24.92	13
II	21.32	13
III	14.12	9
IV	10.65	13
V	8.78	23
VI	8.12	23

Table 6
Load Shedding Locations

Location	Amount (MW)
13	15
9	5
23	10

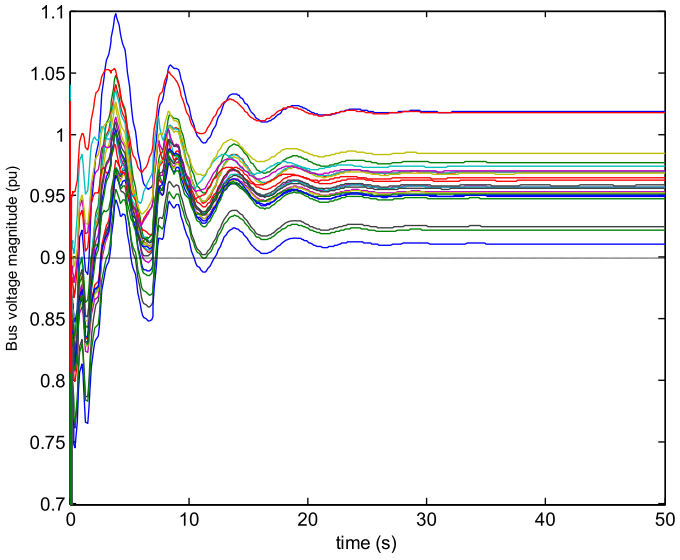

Fig. 14. Voltage improvement after 30 MW load shedding on buses 13, 9 and 23.

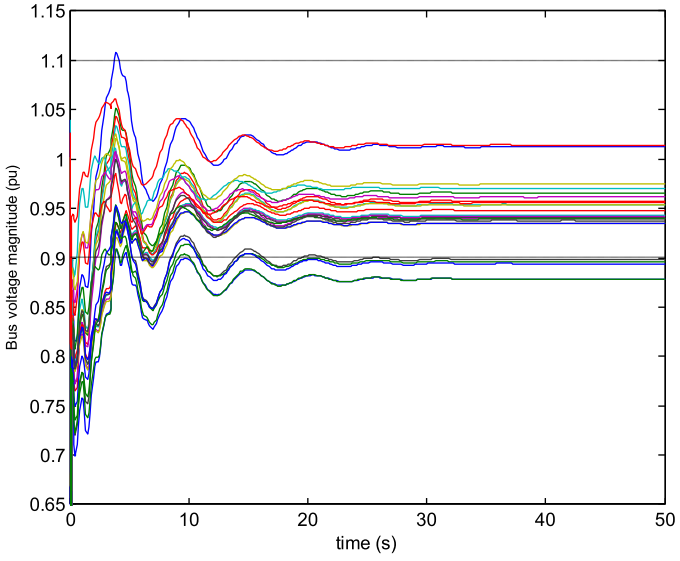

Fig. 15. Voltage performance after 30 MW load curtailment on bus 13.

recommended to perform load shedding on these buses. Table 8 presents a comparison between the results of our proposed methodology and the South Sulawesi system scheme.

The VSM is assessed on the most critical bus after an outage which is bus 12. From Fig. 8, this bus has the lowest voltage magnitude. The base load on bus 12 is 119.2 MW. Fig. 17 shows bus 12 PV curve for the pre-contingency condition with λ^{max} of 1.37 which gives 27% VSM. The complete VSM calculation for all other conditions can be seen in Table 9. From Table 9, the VSM for the post-contingency condition is only -4.17%. The negative value of VSM indicates the system instability,

Table 7
The South Sulawesi System Load Shedding Scheme [31]

No	Substation	Load shedding amount (MW)
1	19	4.44
2	22	4.5
3	4	4.38
4	2	3.27
5	3	1.53
6	24	10.38
7	18	3.15
Total load shedding (MW)	31.64	

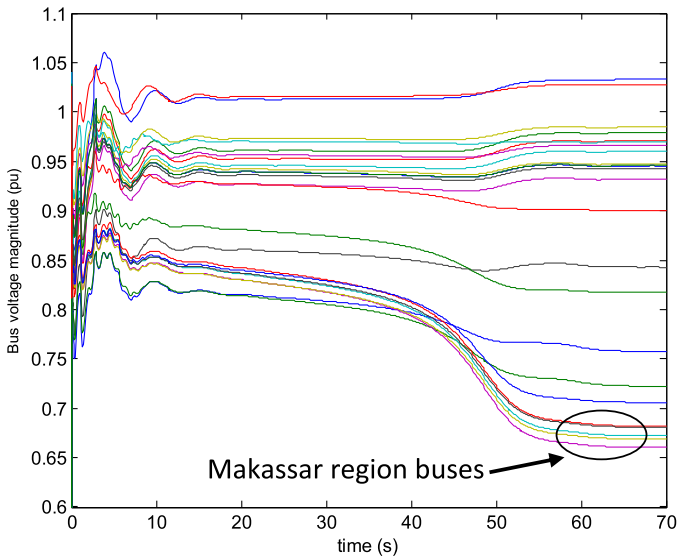

Fig. 16. Voltage performance after load shedding based on the South Sulawesi system scheme.

Table 8
Comparison between Proposed Method and The South Sulawesi Scheme

Scheme	Load shedding Location	Total (MW)	Remarks
Proposed method	13, 9, 23	30	Stable
South Sulawesi scheme (Table VI)	19, 22, 4, 2, 3, 24, 18	31.64	Not stable

therefore precautions are required to preclude the system from voltage collapse. In addition, Table 8 also presents the VSM values for after load shedding conditions. As shown in Fig. 14, the system voltage can improve back to a stable situation after load shedding on the buses based on the proposed method. This is clarified with a positive VSM value of 11.86%. Whereas Fig. 16 shows the system still unstable after load shedding based on the existing scheme from the utility and the VSM is also negative (-2.04%). From this, we can see the results of the VSM calculations are consistent with the dynamic simulation results to prove the robustness of the proposed DVPS based UVLS scheme.

6. Conclusions

This paper recommends a novel under-voltage load shedding design to stabilize the system after large perturbance and to ensure the system secure constraints are fulfilled. The UVLS scheme is designed based on the dynamic sensitivities method that calculates dynamics sensitivity related to system constraints and provides a technique of calculating variations in the system variables with respect to rapid changes in system initial conditions and parameters. In this work, dynamic sensitivity

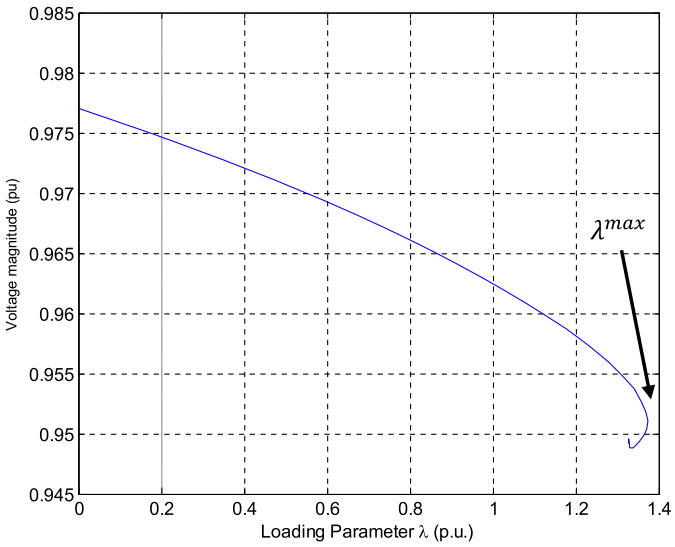

Fig. 17. Pre-contingency PV curve of bus 12.

Table 9
Voltage Stability Margin

Condition	λ^{max}	VSM (%)
Pre-contingency	1.37	27
Post-contingency	0.96	-4.17
Proposed method	1.11	11.86
South Sulawesi scheme	0.98	-2.04

is utilized to verify the minimum amount of load curtailment and to decide the location of load curtailment.

This paper uses the South Sulawesi power system in Indonesia as a case study. The calculation of the dynamic sensitivity index has indicated different buses as load shedding location. The dynamic simulation results as well as the calculations of the voltage stability margin confirm the robustness of the proposed method compared to the load shedding scheme used by the South Sulawesi power system. The dynamic sensitivity index gives convenient information for finding the most appropriate location for load shedding. Finally, it is worth to be clarified that the proposed UVLS methodology consists of a broad method and procedure that can be implemented in designing a more realistic, reliable, and effective approach to dynamic UVLS that takes into account the modeling of loads to any power system. Proper load modeling will give a significant impact on the accuracy of the simulation results.

CRediT authorship contribution statement

Ardiaty Arief: Conceptualization, Methodology, Validation, Writing – original draft. **Muhammad Bachtiar Nappu:** Software, Investigation, Validation. **Zhao Yang Dong:** Conceptualization, Methodology, Supervision, Writing – review & editing.

Declaration of competing interest

The authors declare that they have no known competing financial interests or personal relationships that could have appeared to influence the work reported in this paper.

Acknowledgments

A. Arief and M.B. Nappu gratefully acknowledge the Ministry of Education, Culture, Research and Technology of the Republic of Indonesia for the research grant and support in this work and the Indonesian State Electricity Company (PT. PLN (Persero) AP2B Sistem Sulawesi Selatan) for providing data and discussions. Z.Y. Dong's research is partially supported by the ARC Research hub for integrated energy storage solutions.

References

[1] Z.Y. Dong, P. Zhang, Emerging Techniques in Power System Analysis, Springer, 2009.
[2] Z. Shi, W. Yao, Z. Li, L. Zeng, Y. Zhao, R. Zhang, et al., Artificial intelligence techniques for stability analysis and control in smart grids: Methodologies, applications, challenges and future directions, Appl. Energy 278 (2020), 115733.
[3] M. Begovic, D. Fulton, M.R. Gonzalez, J. Goossens, E.A. Guro, R.W. Haas, et al., Summary of "System Protection and Voltage Stability, IEEE Trans. Power Delivery 10 (1995) 631–638.
[4] T.S.P. Fernandes, J.R. Lenzi, M.A. Mikilita, Load shedding strategies using optimal load flow with relaxation of restrictions, IEEE Trans. Power Syst. 23 (2008) 712–718.
[5] C.M. Affonso, L.C.P. da Silva, F.G.M. Lima, S. Soares, MW and MVar management on supply and demand side for meeting voltage stability margin criteria, IEEE Trans. Power Syst. 19 (2004) 1538–1545.
[6] Y. Wang, I.R. Pordanjani, W. Li, W. Xu, E. Vaahedi, Strategy to minimise the load shedding amount for voltage collapse prevention, IET Generat. Transm. Distribut. 5 (2011) 307–313.
[7] A. Ahmadi, Y. Alinejad-Beromi, A new integer-value modeling of optimal load shedding to prevent voltage instability, Int. J. Electr. Power Energy Syst. 65 (2015) 210–219.
[8] M.M. Hosseini-Bioki, M. Rashidinejad, A. Abdollahi, An implementation of particle swarm optimization to evaluate optimal under-voltage load shedding in competitive electricity markets, J. Power Sources 242 (2013) 122–131.
[9] L.D. Arya, A. Koshti, Anticipatory load shedding for line overload alleviation using Teaching learning based optimization (TLBO), Int. J. Electr. Power Energy Syst. 63 (2014) 862–877.
[10] F. Capitanescu, Enhanced risk-based SCOPF formulation balancing operation cost and expected voluntary load shedding, Electric Power Syst. Res. 128 (2015) 151–155.
[11] D. Chattopadhyay, B.B. Chakrabarti, A preventive/corrective model for voltage stability incorporating dynamic load-shedding, Int. J. Electr. Power Energy Syst. 25 (2003) 363–376.
[12] X. Fu, X. Wang, Determination of load shedding to provide voltage stability, Int. J. Electr. Power Energy Syst. 33 (2011) 515–521.
[13] M. El-Shimy, Stability-based minimization of load shedding in weakly interconnected systems for real-time applications, Int. J. Electr. Power Energy Syst. 70 (2015) 99–107.
[14] Z.A. Hamid, I. Musirin, Optimal Fuzzy Inference System incorporated with stability index tracing: an application for effective load shedding, Expert Syst. Appl. 41 (2014) 1095–1103.
[15] M. Moazzami, M.J. Morshed, A. Fekih, A new optimal unified power flow controller placement and load shedding coordination approach using the Hybrid Imperialist Competitive Algorithm-Pattern Search method for voltage collapse prevention in power system, Int. J. Electr. Power Energy Syst. 79 (2016) 263–274.
[16] V. Tamilselvan, T. Jayabarathi, A hybrid method for optimal load shedding and improving voltage stability, Ain Shams Eng. J. 7 (2016) 223–232.
[17] T. Amraee, A.M. Ranjbar, R. Feuillet, Adaptive under-voltage load shedding scheme using model predictive control, Electric Power Syst. Res. 81 (2011) 1507–1513.
[18] H. Atighechi, P. Hu, S. Ebrahimi, J. Lu, G. Wang, L. Wang, An effective load shedding remedial action scheme considering wind farms generation, Int. J. Electr. Power Energy Syst. 95 (2018) 353–363.
[19] A. Estebsari, E. Pons, T. Huang, E. Bompard, Techno-economic impacts of automatic undervoltage load shedding under emergency, Electric Power Syst. Res. 131 (2016) 168–177.
[20] A. Mahari, H. Seyedi, A wide area synchrophasor-based load shedding scheme to prevent voltage collapse, Int. J. Electr. Power Energy Syst. 78 (2016) 248–257.
[21] A. Arief, Z.Y. Dong, M.B. Nappu, M. Gallagher, Under voltage load shedding in power systems with wind turbine-driven doubly fed induction generators, Electric Power Syst. Res. 96 (2013) 91–100, https://doi.org/10.1016/j.epsr.2012.10.013.
[22] B. Sapkota, V. Vittal, Dynamic VAr planning in a large power system using trajectory sensitivities, IEEE Trans. Power Syst. 25 (2010) 461–469.
[23] IEEE Task Force on Load Representation for Dynamic Performance, Standard load models for power flow and dynamic performance simulation, IEEE Trans. Power Syst. 10 (1995) 1302–1313.
[24] T. Aziz, N.-A. Masood, S.R. Deeba, W. Tushar, C. Yuen, A methodology to prevent cascading contingencies using BESS in a renewable integrated microgrid, Int. J. Electr. Power Energy Syst. 110 (2019) 737–746.
[25] T. Weckesser, H. Jóhannsson, and J. Østergaard, "Impact of model detail of synchronous machines on real-time transient stability assessment," in 2013 IREP Symposium Bulk Power System Dynamics and Control - IX Optimization, Security and Control of the Emerging Power Grid, 2013, pp. 1-9.
[26] P.W. Sauer, M.A. Pai, Power System Dynamics and Stability, Stipes Publising L.L.C, Champaign, Illinois, USA, 2006.
[27] J. Ma, D. Han, R. He, Z. Dong, D.J. Hill, Reducing identified parameters of measurement-based composite load model, IEEE Trans. Power Syst. 23 (2008) 76–83.

[28] W.W. Price, Power System Dynamic Modeling, in: L.L. Grigsby (Ed.), Power System Stability and Control, CRC Press, Taylor and Francis Group, Boca Raton, 2007. Ed., ed.
[29] B. Hua, V. Ajjarapu, A novel online load shedding strategy for mitigating fault-induced delayed voltage recovery, IEEE Trans. Power Syst. 26 (2011) 294–304.
[30] I.A. Hiskens, M.A. Pai, Trajectory sensitivity analysis of hybrid systems, IEEE Trans. Circuit. Syst. I: Fundament. Theory Appl. 47 (2000) 204–220.
[31] PT, PLN (Persero) AP2B Sistem Sulawesi Selatan, Kondisi Kelistrikan Sistem Sulawesi Selatan dan Barat. Makassar, PT. PLN (Persero), Indonesia, 2010.